Available online at www.sciencedirect.com
SCIENCE DIRECT®
Journal of Magnetic Resonance 164 (2003) 369–372
JMR Journal of Magnetic Resonance
www.elsevier.com/locate/jmr

Communication

Double-quantum filtered STMAS

Hyung-Tae Kwak and Zhehong Gan*

Center of Interdisciplinary Magnetic Resonance, National High Magnetic Field Laboratory, Tallahassee, FL 32310, USA

Received 29 May 2003; revised 26 June 2003

Abstract

Double-quantum and double-quantum-filtered satellite-transition magic-angle spinning (STMAS) experiments are proposed. The experiments efficiently convert satellite-transition coherence from single- to double-quantum with a central-transition selective π-pulse. The conversion allows the selection of double-quantum coherence transfer pathways with phase cycling that completely filters out unwanted diagonal and outer satellite-transition peaks. Both experiments are demonstrated with $RbNO_3$ and $AlPO_4$-berlinite as model compounds for obtaining clean STMAS spectra of spins 3/2 and 5/2, respectively.

1. Introduction

Satellite-transition magic-angle spinning (STMAS) experiment offers an alternative to multiple-quantum magic-angle spinning (MQMAS) method to refocus second-order quadrupolar broadening for obtaining high-resolution isotropic NMR spectra of quadrupolar nuclei with half-integer spins [1,2]. The satellite-transition experiment requires very precise magic-angle setting and stable spinning frequencies for a complete refocusing of the first-order quadrupolar interaction but is generally more efficient than the multiple-quantum experiment. It is capable of measuring second-order quadrupole-shielding [3] and third-order quadrupolar interactions [4] that are symmetric with magnetic quantum number m_z. Satellite transitions are also more sensitive to fast molecular motion than the symmetrical multiple-quantum and central transitions that both have zero first-order quadrupolar shift [5]. An undesired feature of STMAS is the presence of central transition–central transition (CT–CT) diagonal peak and peaks from outer satellite transitions of $S > 3/2$ spins. Previously, CT–CT diagonal peaks have been reduced by presaturation [2]. It is also possible to subtract out diagonal peaks by acquiring an additional rotor-desynchronized data set [6,7]. These approaches suffer from either incomplete suppression or loss of a factor of two on spectral sensitivity.

In this communication, a double-quantum (DQ) approach is proposed for filtering out diagonal and outer satellite transition peaks of STMAS spectra. The idea stems from double-quantum filtered (DQF) COSY. By converting coherences from single- to double-quantum, phase cycling that selects double-quantum coherence transfer pathway suppresses dispersive diagonal peaks [8,9]. In the case of quadrupolar nuclei with half-integer spins, the first-satellite transition coherence can be efficiently converted from single- to double-quantum with a central-transition selective π-pulse, while other single-quantum coherences are transferred to other coherence orders. This separation allows the selection of desired first-satellite transition coherence with phase cycling to suppress CT-diagonal and outer satellite transition peaks. The DQF experiment can be easily modified to correlate double-quantum satellite and central transitions that also refocuses the second-order quadrupolar broadening.

Fig. 1a shows the shifted-echo pulse sequence and its matrix representation of various coherence transfer pathways for STMAS experiment of a spin-5/2. The matrix representation is particularly useful for quadrupolar nuclei as it can distinguish coherences with degenerate orders. A spin-S has $2S$ single-quantum transitions all having the same coherence order $p = \pm 1$. In the shifted-echo experiment, coherence transfers

* Corresponding author. Fax: 1-850-644-1366.
E-mail address: gan@magnet.fsu.edu (Z. Gan).

1090-7807/$ - see front matter © 2003 Elsevier Inc. All rights reserved.
doi:10.1016/S1090-7807(03)00246-5

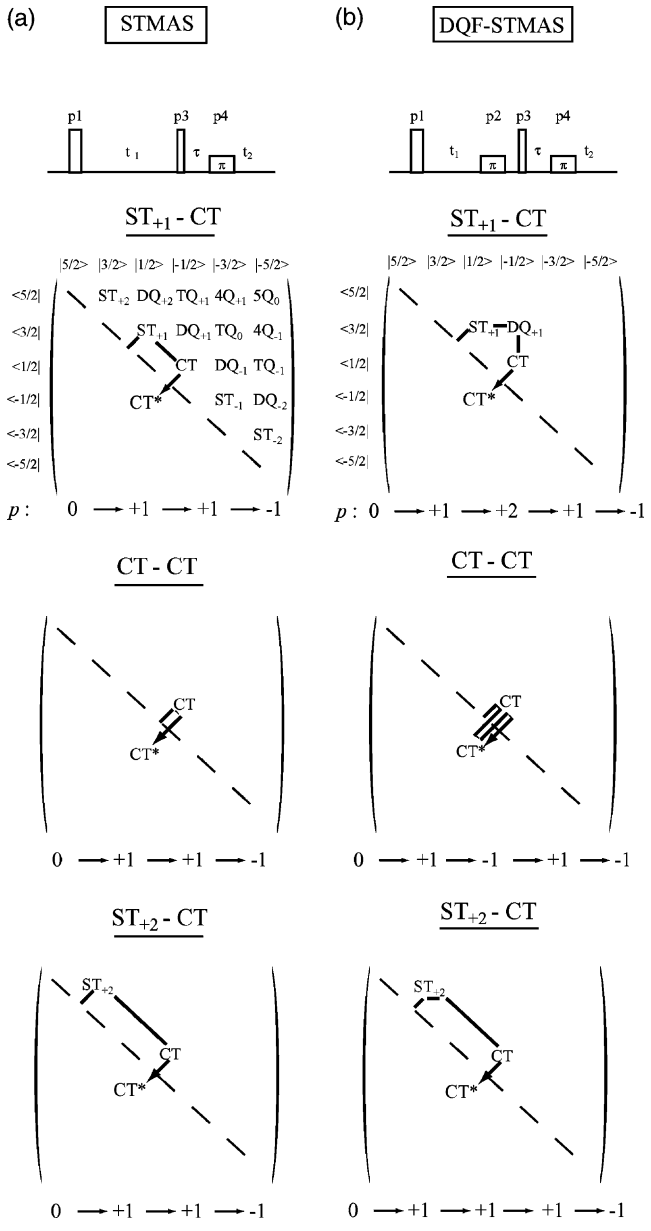

Fig. 1. Shifted-echo pulse sequences and matrix representations of coherence transfer pathways of: (a) STMAS and (b) double-quantum filtered STMAS experiments for spin-5/2. The "walkway" like picture is used to distinguish degenerated coherence transfer pathways in quadrupolar nuclei with half-integer spin.

follow the same pathway p: $0 \rightarrow +1 \rightarrow +1 \rightarrow -1$ for central and other single-quantum satellite transitions. Phase cycling alone cannot separate these degenerated pathways. In the matrix representation picture, these coherence transfers are clearly visualized following different "walkway" like paths.

The key element of double-quantum STMAS experiment is a soft π-pulse prior to the mixing pulse (Fig. 1b). Selective to the central transition, the weak RF pulse inverts $|\pm 1/2\rangle$ states while leaving other spin states undisturbed. As depicted in the density matrix picture, the introduction of the π-pulse converts various single-quantum coherences to different pathways: the central transition coherence is inverted p: $+1 \rightarrow -1$, the first satellite-transition coherence is converted to double-quantum p: $+1 \rightarrow +2$ while outer satellite-transition coherence remains unchanged. This separation allows the selection of double-quantum pathway by phase cycling to filter out undesired $ST_{\pm 2} \rightarrow CT$ and $CT \rightarrow CT$ signals.

Fig. 2 shows the results of the double-quantum filtered STMAS experiment compared with the normal STMAS. The double-quantum scheme is incorporated with commonly used z-filter [10] and shifted-echo [11,12] mixing sequence for spins-3/2 and 5/2, respectively. The STMAS spectra without filtering show strong diagonal peaks and $ST_{\pm 2} \rightarrow CT$ peaks for spin-5/2. These peaks hinder the readability of the spectra especially when taking projections to the isotropic dimension with a spectral shearing. The DQF experiments completely suppress these unwanted peaks yielding clean isotropic projection of STMAS spectra (Fig. 2g).

Fig. 2 also shows double-quantum STMAS sequences and spectra. A simple modification by placing the selective π-pulse before the t_1 period correlates the double-quantum satellite transitions with central transitions $DQ_{\pm 1} \rightarrow CT$. This correlation also refocuses the anisotropic second-order quadrupolar interaction yielding ridge-shaped peaks in the 2D spectra. The slopes of double-quantum peaks are equal to that of single-quantum STMAS plus one: 1/9, 31/24, 73/45, 127/72 for $S = 3/2$, 5/2, 7/2, and 9/2 spins, respectively. The double-quantum STMAS spectra are free of diagonal and outer satellite transition peaks similar to the filter-only single-quantum spectra.

The skyline projections show efficiency comparisons between DQF and normal STMAS experiments. Excitation and mixing pulses for each experiment were optimized iteratively with effective evolution time synchronized with the first rotor period $(p1 + p3)/2 + p2 + \tau_1 + t_1 = \tau_r$. The DQF spectra show ~10% higher intensity for the z-filter sequence ($RbNO_3$) and ~25% lower intensity for the shifted-echo sequence ($AlPO_4$-berlinite) compared to the non-filtered STMAS spectra. The loss in the shifted-echo experiment is due to a combined effect from imperfect π-pulse and different mixing efficiencies between $DQ_{\pm 1} \rightarrow CT$ and $ST_{\pm 1} \rightarrow CT$. For the z-filter experiment, the 10% gain indicates that $DQ_{\pm 1} \rightarrow CT_z$ (central transition polarization) mixing is more efficient than $ST_{\pm 1} \rightarrow CT_z$ mixing. The double-quantum experiment follows the same coherence transfer pathway as the filtering-only experiment and should have the same transfer efficiency. Double-quantum coherences, however, decay faster than single-quantum resulting in broader lines and lower peak intensities along the indirect dimension. The ratio of line width between double- and single-quantum peaks is about 1.5 for both $RbNO_3$ ($S = 3/2$) and $AlPO_4$-berlinite ($S = 5/2$).

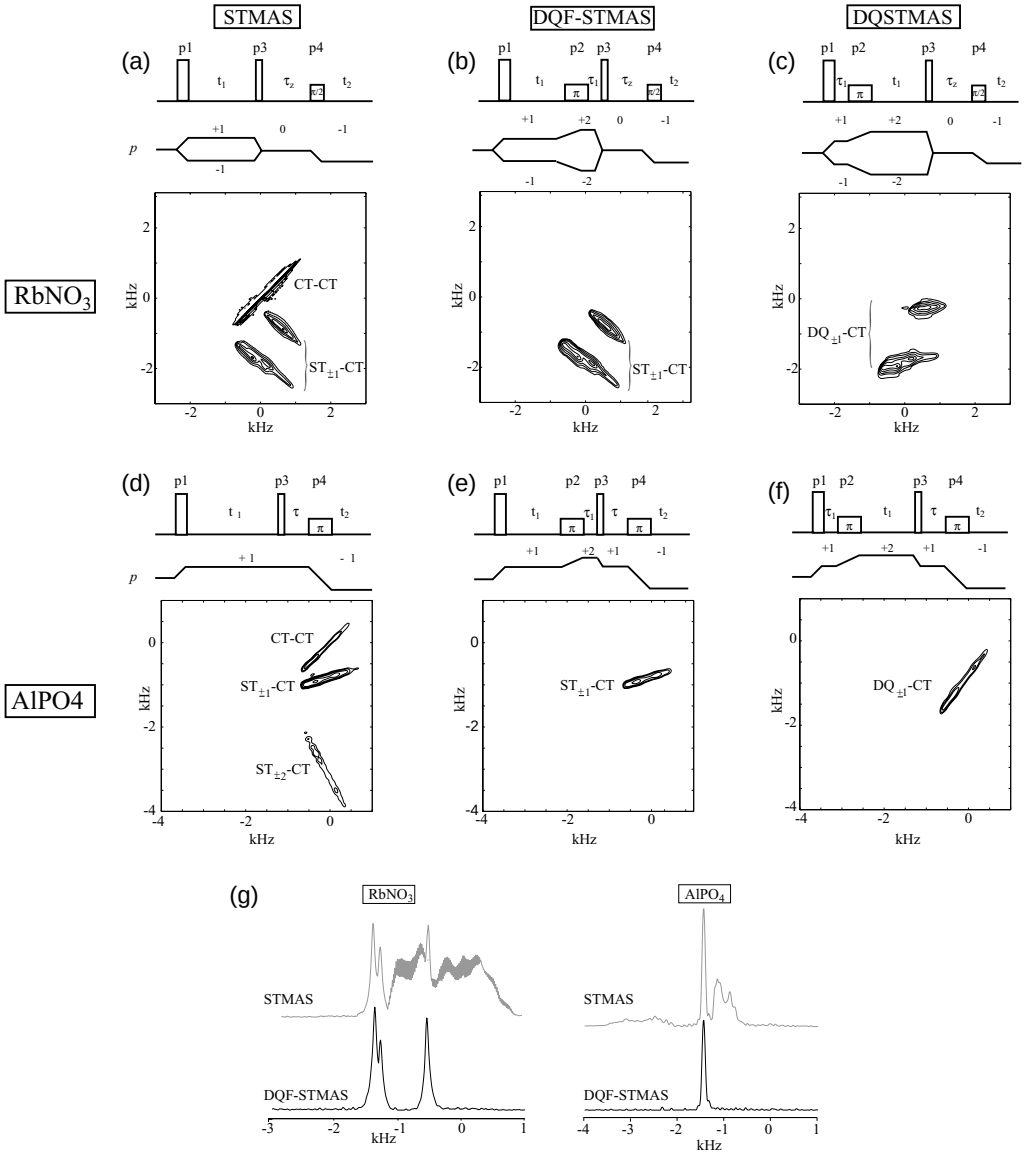

Fig. 2. (a) STMAS, (b) DQF-STMAS, and (c) DQSTMAS experiments with hypercomplex z-filter mixing sequence for ^{87}Rb in $RbNO_3$, (d) STMAS, (e) DQF-STMAS, and (f) DQSTMAS experiments with shifted-echo mixing sequence for ^{27}Al in $AlPO_4$-berlinite, and (g) skyline projections to isotropic dimension after spectral shearing of STMAS (gray) and DQF-STMAS (black) for $RbNO_3$ and $AlPO_4$-berlinite. All experiments were performed on a 600 MHz (^{1}H) Bruker DMX spectrometer using a Bruker 4 mm CPMAS probehead. The pulses of all experiments are defined as $p1$ excitation, $p2$ CT-selective π, $p3$ mixing, and $p4$ detection pulse. The parameters for the ^{87}Rb in $RbNO_3$ experiments were: (a) $p1 = 2.1\,\mu s$, $p3 = 3.4\,\mu s$, $p4 = 9.8\,\mu s$, initial $t_1 = 97.25\,\mu s$ and (b and c) $p1 = 2.1\,\mu s$, $p2 = 19.6\,\mu s$, $p3 = 1.6\,\mu s$, $p4 = 9.8\,\mu s$, initial $t_1 = 74.45\,s$, $\tau_1 = 4\,\mu s$, $|\omega_1/2\pi| \approx 74$ kHz (for $p1$ and $p3$), $|\omega_1/2\pi| \approx 13$ kHz (for $p2$ and $p4$) with recycle delay of 0.1 s for each of 128 t_1 increments. The parameters for the ^{27}Al in $AlPO_4$-berlinite experiments were (d) $p1 = 1.7\,\mu s$, $p3 = 1\,\mu s$, $p4 = 14\,\mu s$, initial $t_1 = 98.65\,\mu s$ and (e and f) $p1 = 1.7\,\mu s$, $p2 = 14\,\mu s$, $p3 = 0.7\,\mu s$, $p4 = 14\,\mu s$, initial $t_1 = 80.8\,\mu s$, $\tau_1 = 4\mu s$, $|\omega_1/2\pi| \approx 76$ kHz (for $p1$ and $p3$), $|\omega_1/2\pi| \approx 12$ kHz (for $p2$ and $p4$) with recycle delay of 0.5 s for each of 32 t_1 increments. The z-filter delay τ_z and the shifted-echo delay τ were set to 0.14 and 4 ms, respectively. The first t_1 and 100 μs increment are synchronized with 10 kHz MAS spinning rate (see text). A 16-step phase cycle was used to select the desired coherence transfer pathway in (b) and (c): $p1$, $+x$, $-x(\cos) + y$, $-y(\sin)$; $p2$, $2(+x)$ $2(-x)$; $p3$, $4(+x)$ $4(+y)$ $4(-x)$ $4(-y)$; and receiver phase $= p1 + p2 - 2p3$. A 64-step phase cycle was used in (e) and (f): $p1$, $+x$, $-x$, $+y$, $-y$; $p2$, $4(+x)$ $4(+y)$ $4(-x)$ $4(-y)$; $p3$, $16(+x)$ $16(+y)$ $16(-x)$ $16(-y)$; and receiver phase $= -p1 - p2 + p3$. A 4-step phase cycling for $p4$ can be added if needed. $RbNO_3$ has three crystallographically different sites with C_q of 1.83, 1.91, and 2.39 MHz and η_q of 0.12, 1.00, and 0.48, respectively. $AlPO_4$-berlinite has a single site with C_q of 4.067 MHz and η_q of 0.35.

Precise magic-angle setting and rotor synchronization are essential to STMAS experiment for the complete refocusing of the large first-order quadrupolar interaction. It is important to note that the double-quantum satellite transitions are subject to the same first-order quadrupolar shift as the single-quantum satellite transitions, therefore the insertion of the π-pulse does not affect the first-order quadrupolar evolution. Satellite transition rotational echoes form at multiples of the rotor period after the excitation pulse. In both DQ and DQF experiments, the

excitation and mixing pulses ($p1$ and $p3$ in Fig. 2) must be rotor synchronized when setting up the initial t_1 and time increments of the 2D experiments $(p1 + p3)/2 + p2 + \tau_1 + t_1 = n\tau_r$. The finite length of all three pulses and the short delay τ_1 in the sequences need be included for the rotor-synchronization.

The rotor synchronization also plays a role in the efficient filtering of diagonal and outer satellite transition peaks. The undesired signals from CT and $ST_{\pm 2}$ can leak through the double-quantum filter because the soft π-pulse can induce some coherences transfer to double-quantum despite of low efficiencies. The central transition has zero first-order quadrupolar shift and the outer satellite transitions $ST_{\pm 2}$ have a first-order shift twice as that of $ST_{\pm 1}$. Therefore these coherences are not refocused at the mixing pulse with the t_1 evolution time carefully chosen for the rotor-synchronization of the first-satellite transition coherence. The combined effects from low coherence transfer efficiencies and rotor-desynchronization of these leak-through coherences explain the superb performance on the suppression of the CT and $ST_{\pm 2}$ peaks as shown in Fig. 2g.

In conclusion, the double-quantum version of STMAS experiment has been demonstrated with two commonly used mixing sequences to completely filter out undesired peaks in STMAS spectra. The double-quantum conversion can be achieved by a central-transition selective π-pulse with no or a little loss of sensitivity. The new sequences can be used to acquire both single- and double-quantum STMAS spectra. The single- and double-quantum experiments complement with the triple-quantum experiment for obtaining high-resolution spectra and measuring various high-order and motional effects of quadrupolar nuclei.

Acknowledgments

This work is supported by the National High Magnetic Field Laboratory through National Science Foundation Cooperative Agreement DMR0084173 and by the State of Florida.

References

[1] L. Frydman, J.S. Harwood, Isotropic spectra of half-integer quadrupolar spins from bidimensional magic-angle-spinning NMR, J. Am. Chem. Soc. 117 (1995) 5367–5368.
[2] Z.H. Gan, Isotropic NMR spectra of half-integer quadrupolar nuclei using satellite transitions and magic-angle spinning, J. Am. Chem. Soc. 122 (2000) 3242–3243.
[3] S. Wi, S.E. Ashbrook, S. Wimperis, L. Frydman, Second-order quadrupole-shielding effects in magic-angle spinning solid-state nuclear magnetic resonance, J. Chem. Phys. 118 (2003) 3131–3140.
[4] Z.H. Gan, P. Srinivasan, J.R. Quine, S. Steuernagel, B. Knott, Third-order effect in solid-state NMR of quadrupolar nuclei, Chem. Phys. Lett. 367 (2003) 163–169.
[5] S.E. Ashbrook, S. Antonijevic, A.J. Berry, S. Wimperis, Motional broadening: an important distinction between multiple-quantum and satellite-transition MAS NMR of quadrupolar nuclei, Chem. Phys. Lett. 364 (2002) 634–642.
[6] C. Huguenard, F. Taulelle, B. Knott, Z.H. Gan, Optimizing STMAS, J. Magn. Reson. 156 (2002) 131–137.
[7] K.J. Pike, S.E. Ashbrook, S. Wimperis, Two-dimensional satellite-transition MAS NMR of quadrupolar nuclei: shifted echoes, high-spin nuclei and resolution, Chem. Phys. Lett. 345 (2001) 400–408.
[8] U. Piantini, O.W. Sorensen, R.R. Ernst, Multiple quantum filters for elucidating NMR coupling networks, J. Am. Chem. Soc. 104 (1982) 6800–6801.
[9] G. Bodenhausen, H. Kogler, R.R. Ernst, Selection of coherence-transfer pathways in NMR pulse experiments, J. Magn. Reson. 58 (1984) 370–388.
[10] J.P. Amoureux, C. Fernandez, S. Steuernagel, *Z* filtering in MQMAS NMR, J. Magn. Reson. Ser. A 123 (1996) 116–118.
[11] P.J. Grandinetti, J.H. Baltisberger, A. Llor, Y.K. Lee, U. Werner, M.A. Eastman, A. Pines, Pure-absorption-mode lineshapes and sensitivity in 2-dimensional dynamic-angle spinning NMR, J. Magn. Reson. Ser. A 103 (1993) 72–81.
[12] D. Massiot, B. Touzo, D. Trumeau, J.P. Coutures, J. Virlet, P. Florian, P.J. Grandinetti, Two-dimensional magic-angle spinning isotropic reconstruction sequences for quadrupolar nuclei, Solid State Nucl. Mag. Reson. 6 (1996) 73–83.